

## **Semi-automatic aerotriangulation with digital OEEPE image data at the Digital Photogrammetric Station DIPS II of ETH Zurich**

Thomas Kersten, Dirk Stallmann

Institute of Geodesy and Photogrammetry, Swiss Federal Institute of Technology  
ETH-Hoenggerberg, CH-8093 Zurich, Switzerland

Phone: +41 1 633 3287, Fax: +41 1 633 1101, e-mail: [thomas, dirk]@p.igp.ethz.ch

### **Abstract**

With the development of higher-resolution scanners, faster image-handling capabilities, and higher-resolution screens, digital photogrammetric workstations promise to rival conventional analytical plotters in functionality, i.e. degree of automation in data capture and processing, and in accuracy. The availability of high quality digital image data offers the capability to perform accurate semi-automatic or automatic triangulation of digital aerial photo blocks on digital photogrammetric workstations instead of analytical plotters.

In this paper, we present investigations using hard- and software, and results of the Institute of Geodesy and Photogrammetry, ETH Zurich on the OEEPE test project "Aerotriangulation using digitized images". For this international experiment the delivered two data sets of digital images were processed with components of the Digital Photogrammetric Station DIPS II using own software packages. The measurement of the fiducial marks, signalised and natural tie points was performed by least squares template and image matching. The self-calibrating bundle adjustment yielded an estimated standard deviation of the image coordinates of about 1/4th of the pixel size for both data sets. An empirical accuracy of  $\mu_{xy} = 26$  mm and  $\mu_z = 38$  mm was obtained in object space from the check points with the 15  $\mu$ m digital data set.

### **1 Hardware and software components**

For the investigations with the test data, basic hardware components of the Digital Photogrammetric Station DIPS II (*Grün/Beyer, 1990*) of the Institute of Geodesy and Photogrammetry were used. DIPS II consists of 2 file servers and 16 Sun workstations linked to each other via Ethernet with some external components for digital image acquisition and output. DIPS II serves as a platform for all research and development projects of the Institute. At the current stage, a total of 15 GByte for is available data storage. For the OEEPE test 2 GByte could be effectively used.

The relevant used programs, which are developed in the Institute, are summarized in the following:

- A viewing tool for the display of the images, manual measurement of image points, and extraction of Regions Of Interest (ROIs) from images.
- A Least Squares Matching (LSM) tool for measuring fiducial marks, signalised and natural points.
- A program for bundle adjustment with self calibration and analysis of the observation data.
- Different programs for affine transformations, corrections of the image point observations (earth curvature, refraction, and distortion), changing rasterfile and data formats, etc.

### **2 Preprocessing of digital image data**

For point positioning in aerial triangulation only parts of the whole image are interesting for measurements, i.e. fiducial marks for transformations into image coordinates, signalised points with known 3-D coordinates for transformations into object space, and tie points along strip and across strip direction for reliable connection of the images. The input and output of large digital images (i.e. 256 Mbyte) and their display require large disk storage and consume long I/O time. Due to these

aspects, the concept in our investigations was to use only ROIs of the images for the measurements. Therefore, patches of the eight fiducial marks, all visible signalised points and selected tie points were extracted automatically in each digital image using approximate pixel coordinates provided by the pilot center or measured manually before extraction. For the extraction the images were temporarily stored on disk. For all ROIs no image enhancement was performed.

The patch size of each extracted ROI was  $64 \times 64$  pixels ( $30 \mu\text{m}$ ) and  $128 \times 128$  pixels ( $15 \mu\text{m}$ ). Only for tie points of the  $30 \mu\text{m}$  image data, which were manually selected in the six ‘‘von Gruber’’ positions in each image, the patch size was  $512 \times 512$  pixels. Excluding fiducial marks the average number of image patches per image was 25.

### 3 Mono image point measurement by template and image matching

The image point measurement for all points (fiducials, signalised and tie points) was performed by matching in the patches. The used algorithm is known as constrained Least Squares image Matching (LSM), which allows point measurements with subpixel accuracy, and is described in *Grün/Baltsavias (1988)*. The matching was performed interactively with the LSM tool using a window-based interface to the algorithm. This allows all algorithm parameters (e.g. patch size etc.) to be set to optimum values for a particular matching problem, plus assessment of the result by visual inspection for quality control: if a point could not be matched satisfactorily with the chosen parameters, then an alternative optimum set was found - usually a smaller or larger patch size or restricted image shaping transformation.

For matching fiducial marks and signalised points, artificial templates were created. The fiducial marks were well defined and the matching could be performed without problems. In Figure 1 the large images show the matching between template and patch indicating the initial position as a point and the final solution as a cross, while the lower small images depict visually the matching result.

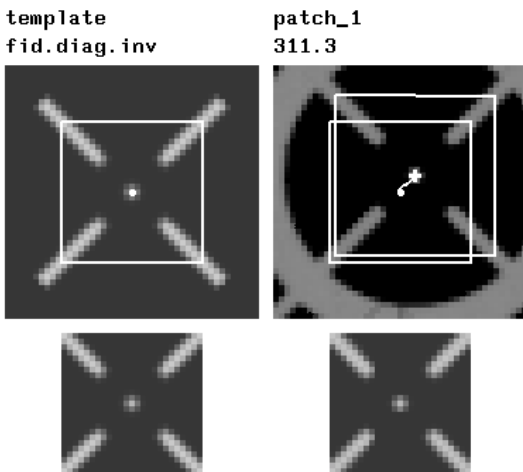


Figure 1: Template matching of fiducial marks ( $30 \mu\text{m}$  image data)

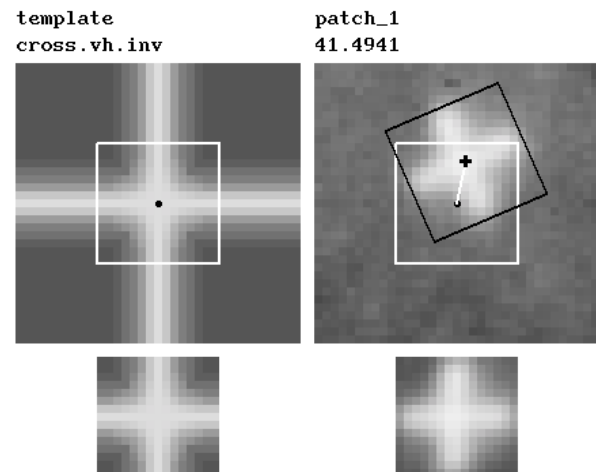


Figure 2: Template matching of signalized points ( $15 \mu\text{m}$  image data)

The signalised points were not so straightforward to match in the  $30 \mu\text{m}$  image patches as their images show a great variety in shape and contrast. On the average, the targets occupied a square of 5-7 pixels ( $30 \mu\text{m}$ ) resp. 10-14 pixels ( $15 \mu\text{m}$ ).

The quality of the  $30 \mu\text{m}$  digital image material did not allow template matching with an affine transformation. Thus, to obtain an acceptable result, the signalised points were matched with two translation parameters using a patch size of  $7 \times 7$  pixels. In the high resolution patches all targets could be matched with the same template using a conformal transformation and an average patch size of  $15 \times 15$  pixels. Figure 2 shows the template matching of one target. In total, 257 targets

(minimum 3 and maximum 16 points per image) were matched. In the center of the block the same signalled points could be measured in up to six different images, while at the perimeter of the block the points have only two rays.

In the matching procedure of the tie points one natural point was used as the template point to be located in the other ROIs. Well defined points were mostly selected in the patches as natural tie points, in general, points in flat areas, and the matching could be done without problems. For reliability reasons two tie points were matched in each 512 x 512 patch. In total, 460 tie points in the 30  $\mu\text{m}$  images and 442 in the 15  $\mu\text{m}$  images were matched for the whole image data set. The image matching of four tie points in two strips is illustrated in Figure 3.

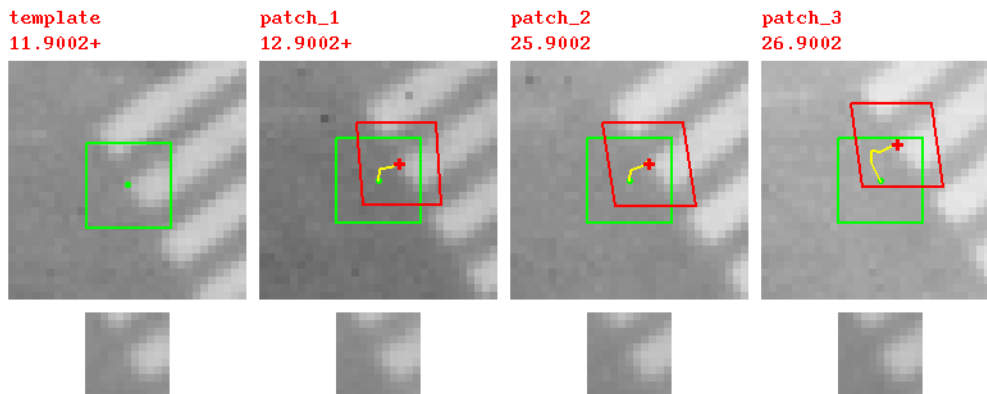


Figure 3: Image Matching of four tie points (30  $\mu\text{m}$  image data)

#### 4 Bundle block adjustment

Before the adjustment the pixel coordinates were transformed into image coordinates by an affine transformation and also a priori corrected for radial lens distortion, refraction, and earth curvature. The adjustment of these reduced image coordinates was performed with the software package BUN, which is a collection of more than 40 programs, separated in four parts, namely preprocessing of data, bundle adjustment with self calibration, analysis of results, and plot facilities. The mathematical background of the bundle adjustment in this program is described in *Grün (1976)*. The bundle adjustment program, the main part of BUN, allows the automatic computation of initial values including checks for gross errors and their automatic elimination at that stage. For the compensation of systematic errors in aerial photos the 12 Additional Parameters (AP) of *Ebner (1976)* or the 44 APs of *Grün (1978)* can be used optionally in the adjustment. For the digital OEEPE test image data both additional parameter sets were used.

The results from the bundle adjustment are summarized in Table 3 of Appendix B. In Table 4 of Appendix B the empirical accuracy from check points is summarized.

#### 5 Conclusions, further works, criticism

In the investigations for the OEEPE test project a standard deviation of image coordinates of 0.25 pixel was obtained for the low and high resolution digital image data. The aerotriangulation of each digital data set was performed in less than 50 hours. Detailed descriptions of these investigations are given in *Kersten/Stallmann (1994)*. At the current state the used procedure can be optimised as summarised in the following, to increase the degree of automation in aerial triangulation and to improve the efficiency in comparison to aerotriangulation using analytical plotters:

- Optimization of the interface between different software modules
- Use of tiled images and image pyramids

- Automation of interior and relative orientation
- Introduction of on-line triangulation by sequential estimation
- Introduction of blunder detection by data snooping

Finally, some critical aspects on the overall procedure of the OEEPE test are summarised:

- The digital test image data were delivered including some radiometric errors as described in *Kersten/Stallmann (1994)*, which could be attributed to insufficient scanner calibration.
- The targets of the signalised points are not very suitable for measurements by template matching. Signalisation with disks might give better results.
- The control point configuration was not optimal for a reliable and geometrically stable bundle adjustment. Additional height control in the block center would stabilize the block geometry.
- The given a priori standard deviation of the control points was not very accurate compared with the photo scale of this data. This can seriously disturb a clear and conclusive analysis of the empirical results.

## 6 References

- EBNER, H., 1976. Self Calibrating Block Adjustment. *Int. Archives of Photogrammetry and Remote Sensing*, Vol. 21, Part 3, Invited Paper, Commission III, ISP Congress, Helsinki.
- GRÜN, A., 1976. Die simultane Kompensation systematischer Fehler mit dem Münchner Bündelprogramm MBOP. *International Archives of Photogrammetry and Remote Sensing*, Vol. 21, Part 3, Presented Paper, Commission III/1, ISP Congress, Helsinki.
- GRÜN, A., 1978. Experiences with Self-Calibrating Bundle Adjustment. Presented Paper, *ASP Convention, Washington D.C.*, Febr./March.
- GRÜN, A., BALTSAVIAS, E.P., 1988. Geometrically Constrained Multiphoto Matching. *Photogrammetric Engineering and Remote Sensing*, 54(5), pp. 633-641.
- GRÜN, A., BEYER, H., 1990. DIPS II - Turning a Standard Computer Workstation into a Digital Photogrammetric Station. *Int. Archives of Photogrammetry and Remote Sensing*, Vol. 28, Part. 2, pp. 247-255 and *ZPF - Zeitschrift für Photogrammetrie und Fernerkundung*, No. 1/91, pp. 2-10.
- KERSTEN, TH., STALLMANN, D., 1994. Aerotriangulation with Digital OEEPE Test Image Data - Contribution of the IGP (ETH Zurich) to the OEEPE Test. *Internal report for the OEEPE Workshop on Digital Methods in Aerial Triangulation*, Helsinki-Espoo, Finland, May 8-10.

## APPENDIX B

| Case | Pix. size | Ctrl. D/S | AP Y/N | $\hat{\sigma}_0$ [ $\mu\text{m}$ ] | Ground |    |     | Camera |       |       |        |          |          |
|------|-----------|-----------|--------|------------------------------------|--------|----|-----|--------|-------|-------|--------|----------|----------|
|      |           |           |        |                                    | N      | E  | H   | $N_0$  | $E_0$ | $H_0$ | $\phi$ | $\omega$ | $\kappa$ |
| 1    | 15        | D         | N      | 3.9                                | 18     | 16 | 39  | 45     | 47    | 29    | 4.7    | 4.1      | 1.5      |
| 2    | 15        | D         | Y/12   | 3.8                                | 19     | 16 | 40  | 47     | 50    | 30    | 4.9    | 4.2      | 1.5      |
| 3    | 15        | D         | Y/44   | 3.8                                | 19     | 16 | 42  | 53     | 57    | 32    | 5.6    | 4.8      | 1.6      |
| 4    | 15        | S         | N      | 3.8                                | 27     | 23 | 44  | 59     | 52    | 33    | 4.8    | 4.8      | 1.9      |
| 5    | 15        | S         | Y/12   | 3.7                                | 32     | 27 | 46  | 65     | 61    | 38    | 5.7    | 5.0      | 2.1      |
| 6    | 15        | S         | Y/44   | 3.8                                | 33     | 29 | 65  | 74     | 101   | 58    | 10.1   | 5.9      | 2.3      |
| 7    | 30        | D         | N      | 7.7                                | 34     | 30 | 74  | 82     | 87    | 53    | 8.6    | 7.4      | 2.7      |
| 8    | 30        | D         | Y/12   | 7.5                                | 36     | 30 | 75  | 87     | 92    | 55    | 9.1    | 7.8      | 2.7      |
| 9    | 30        | D         | Y/44   | 7.6                                | 38     | 32 | 82  | 107    | 107   | 62    | 10.5   | 9.7      | 3.1      |
| 10   | 30        | S         | N      | 7.4                                | 50     | 42 | 82  | 108    | 95    | 63    | 8.9    | 8.8      | 3.4      |
| 11   | 30        | S         | Y/12   | 7.3                                | 61     | 49 | 87  | 123    | 113   | 72    | 10.7   | 9.3      | 4.1      |
| 12   | 30        | S         | Y/44   | 7.5                                | 65     | 54 | 125 | 108    | 149   | 108   | 12.0   | 19.4     | 4.6      |

Table 3: Theoretical precision of unknown ground coordinates [mm] and orientation parameters [mm, mgon]: Results from ETH Zurich

| Case | Pix. size | Ctrl. D/S | AP Y/N | $\hat{\sigma}_0$ [ $\mu\text{m}$ ] | Ground |    |    |
|------|-----------|-----------|--------|------------------------------------|--------|----|----|
|      |           |           |        |                                    | N      | E  | H  |
| 1    | 15        | D         | N      | 3.9                                | 35     | 29 | 42 |
| 2    | 15        | D         | Y/12   | 3.8                                | 27     | 25 | 38 |
| 3    | 15        | D         | Y/44   | 3.8                                | 28     | 24 | 38 |
| 4    | 15        | S         | N      | 3.8                                | 43     | 31 | 48 |
| 5    | 15        | S         | Y/12   | 3.7                                | 29     | 27 | 63 |
| 6    | 15        | S         | Y/44   | 3.8                                | 38     | 30 | 42 |
| 7    | 30        | D         | N      | 7.7                                | 74     | 38 | 69 |
| 8    | 30        | D         | Y/12   | 7.5                                | 73     | 32 | 66 |
| 9    | 30        | D         | Y/44   | 7.6                                | 73     | 32 | 66 |
| 10   | 30        | S         | N      | 7.4                                | 169    | 57 | 66 |
| 11   | 30        | S         | Y/12   | 7.3                                | 160    | 43 | 63 |
| 12   | 30        | S         | Y/44   | 7.5                                | 173    | 39 | 67 |

Table 4: Empirical accuracy of ground points [mm] from check points  
Results from ETH Zurich